Unified Description of Electron Transfer and Nonlinear Optical Spectroscopy

SHAUL MUKAMEL*,† and YI JING YAN

Department of Chemistry, University of Rochester, Rochester, New York 14627

Received February 1, 1989 (Revised Manuscript Received May 15, 1989)

I. Introduction

Solvent motions and relaxation processes play a crucial role in the dynamics of reaction rates[1-17] and in determining molecular linear and nonlinear optical properties. Electron-transfer rates are dominated by the solvent dielectric fluctuations,[1-11] whereas isomerization reactions[12-17] are directly affected by solvent friction. Optical line shapes of polyatomic molecules in solution provide a direct probe for the interaction between the solvent and the solute.[18-26] The solvent-induced spectral shifts and line broadening, and their temporal evolution, reflect the intermolecular forces resulting in electronic and vibrational relaxation processes. Recent developments in nonlinear optical spectroscopy, in particular the successful application of femtosecond laser pulses,[22] provide a direct probe for elementary photophysical and photochemical processes. The dynamics and relaxation processes in semiconductors,[27] solvated dye molecules,[19-23] elementary reaction events,[24] and the solvated electron[28-31] were monitored with remarkable temporal and spectral resolution. In this Account we present a semiclassical theoretical framework[32-35] that provides a unified description of molecular rate processes and nonlinear optical spectroscopy. Considerable progress was made recently in understanding the elementary electron-transfer processes in the photosynthetic reaction center.[36] The interpretation of pump–probe and photon echo measurements conducted on this system and their relationship with the electron transfer is an interesting puzzle. The concepts presented here may contribute toward clarifying the relationships among the optical and the electron-transfer measurements in this complex system.

The connection between rate theories and optical line shapes may be understood as follows: Reaction rates may be calculated by starting with a nonadiabatic (two-state) model and expanding the rate perturbatively in the nonadiabatic coupling V. Optical line shapes are usually calculated by expanding the polarization in powers of the electric field E. Both expansions are expressed in terms of correlation functions. To lowest order (V^2), the nonadiabatic rate is given by the Fermi

Shaul Mukamel received the Ph.D. degree in chemistry in 1976 from Tel Aviv University. He conducted postdoctoral research at the Massachusetts Institute of Technology and the University of California, Berkeley. In 1982 he joined the faculty at the University of Rochester, where he is currently a professor of chemistry. His research interests include theoretical studies of molecular nonlinear optical processes, spectral line broadening, transport of excitations in disordered systems, electron transfer and localization, molecular relaxation, and nonequilibrium statistical mechanics. He was an Alfred P. Sloan Fellow and a Camille and Henry Dreyfus Teacher-Scholar. He is a fellow of the American Physical Society and of the Optical Society of America.

Yi Jing Yan was born in Fuzhou, China, in 1955. He received his B.S. degree in chemistry from Fudan University in 1982 and his Ph.D. degree in 1988 from the University of Rochester. He is now a postdoctoral fellow at the University of Rochester. His research interests are in theoretical chemical physics, molecular dynamics of chemical reactions, and optical spectroscopy of polyatomic molecules in condensed phases.

† Camille and Henry Dreyfus Teacher-Scholar.

(1) Makinen, M. W.; Schichman, S. A.; Hill, S. C.; Gray, H. B. *Science* **1983**, *222*, 929.
(2) Closs, G. L.; Miller, J. R. *Science* **1988**, *240*, 440.
(3) McLendon, G. *Acc. Chem. Res.* **1988**, *21*, 160.
(4) Hicks, J.; Vandersoll, M.; Sitzmann, E. V.; Eisenthal, K. B. *Chem. Phys. Lett.* **1987**, *135*, 413.
(5) Kosower, E. M.; Huppert, D. *Annu. Rev. Phys. Chem.* **1986**, *37*, 127.
(6) Hopfield, J. J. *Biophys. J.* **1977**, *18*, 311.
(7) Jortner, J. *Biochem. Biophys. Acta* **1980**, *594*, 193.
(8) Marcus, R. A.; Sutin, N. *Biochem. Biophys. Acta* **1985**, *811*, 275. Sumi, H.; Marcus, R. A. *J. Chem. Phys.* **1986**, *84*, 4894.
(9) Rips, I.; Jortner, J. *J. Chem. Phys.* **1987**, *87*, 2090.
(10) Zusman, L. D. *Chem. Phys.* **1980**, *49*, 295; **1983**, *80*, 29. Zusman, L. D.; Helman, A. B. *Opt. Spectrosc. (Engl. Transl.)* **1982**, *53*, 248. Yakobson, B. I.; Burshtein, A. I. *Chem. Phys.* **1980**, *49*, 385.
(11) Onuchic, J. N.; Beratan, D. N.; Hopfield, J. J. *J. Phys. Chem.* **1986**, *90*, 3707.
(12) Barbara, P. F.; Jarzeka, W. *Acc. Chem. Res.* **1988**, *21*, 195.
(13) Ben Amotz, D.; Harris, C. B. *J. Chem. Phys.* **1987**, *86*, 4856, 5433.
(14) Kramers, H. A. *Physica* **1940**, *7*, 284.
(15) Waldeck, D.; Fleming, G. R. *J. Phys. Chem.* **1981**, *85*, 2614.
(16) Lee, M.; Bain, A. J.; McCarthy, P. J.; Ham, C. H.; Haseltine, J. N.; Smith, A. B.; Hochstrasser, R. M. *J. Chem. Phys.* **1986**, *85*, 4341.
(17) Northrup, S. H.; Hynes, J. T. *J. Chem. Phys.* **1980**, *73*, 2700. Hynes, J. T. *Annu. Rev. Phys. Chem.* **1985**, *36*, 573. Hynes, J. T. *J. Phys. Chem.* **1986**, *90*, 3701.
(18) Berg, M.; Walsh, C. A.; Narashimhare, L. R.; Littau, K. A.; Fayer, M. D. *J. Chem. Phys.* **1988**, *88*, 1564.
(19) Yan, Y.; Nelson, K. *J. Chem. Phys.* **1987**, *87*, 6240, 6257. Yan, Y. X.; Cheng, L. T.; Nelson, K. *Advances in Nonlinear Spectroscopy*; Clark, R. J. H., Hester, R. E., Eds.; Wiley: New York, 1988. McMorrow, D.; Lotshaw, W. T.; Kenney-Wallace, G. A. *IEEE J. Quantum Electron.* **1988**, *QE-24*, 443.
(20) Rosker, M. J.; Wise, F. W.; Tang, C. L. *Phys. Rev. Lett.* **1986**, *57*, 321. Walmsley, I. A.; Mitsunaga, M.; Tang, C. L. *Phys. Rev. A* **1988**, *38*, 4681.
(21) Maroncelli, M.; Fleming, G. *J. Chem. Phys.* **1988**, *89*, 875; **1987**, *86*, 6221.
(22) Brito Cruz, C. H.; Fork, R. L.; Knox, W.; Shank, C. V. *Chem. Phys. Lett.* **1986**, *132*, 341. Mathies, R. A.; Brito Cruz, C. H.; Pollard, W. T.; Shank, C. V. *Science* **1988**, *240*, 777.
(23) Chesnoy, J.; Mokhtari, A. *Phys. Rev. A* **1988**, *38*, 3566. Saikan, S. *Phys. Rev. A* **1988**, *38*, 4669.
(24) Zewail, A. H.; Bernstein, R. B. *Chem. Eng. News* **1988**, *66*, 24.
(25) Mazurenko, Y. T.; Udaltsov, V. S. *Opt. Spectrosc. (Engl. Transl.)* **1987**, *44*, 417; **1978**, *45*, 765.
(26) Mukamel, S. *Phys. Rev. A* **1983**, *28*, 3480. Boyd, R. W.; Mukamel, S. *Ibid.* **1984**, *29*, 1973. Yan, Y. J.; Fried, L.; Mukamel, S. *J. Phys. Chem.*, to be published.
(27) *Optical Nonlinearities and Instabilities in Semiconductors*; Haug, H., Ed.; Academic: New York, 1988.
(28) Migus, A.; Gauduel, Y.; Martin, J. L.; Antonetti, A. *Phys. Rev. Lett.* **1987**, *58*, 1559.
(29) Schnitker, J.; Rossky, P. J. *J. Chem. Phys.* **1987**, *86*, 3462, 3471.
(30) Coker, D. F.; Berne, B. J.; Thirumalai, D. *J. Chem. Phys.* **1987**, *86*, 5689.
(31) Barnett, R. N.; Landman, U.; Cleveland, C. L.; Jortner, J. *J. Chem. Phys.* **1988**, *88*, 4421, 4429.
(32) Mukamel, S. *Adv. Chem. Phys.* **1988**, *70*, Part I, 165. Mukamel, S.; Loring, R. F. *J. Opt. Soc. Am. B* **1986**, *3*, 595.
(33) Yan, Y. J.; Mukamel, S. *J. Chem. Phys.* **1988**, *89*, 6160.
(34) Loring, R. F.; Yan, Y. J.; Mukamel, S. *J. Chem. Phys.* **1987**, *87*, 5840.
(35) Sparpaglione, M.; Mukamel, S. *J. Chem. Phys.* **1988**, *88*, 3263, 4300. Yan, Y. J.; Spargaglione, M.; Mukamel, S. *J. Phys. Chem.* **1988**, *92*, 4842.

0001-4842/89/0122-0301$01.50/0

golden rule;[6,7] the optical response to first order in E (e.g., the absorption line shape) is given by the linear susceptibility $\chi^{(1)}$. Both quantities are related to a two-time correlation function of the solvent. In the next order (V^4), the rate is related to a four-point correlation function.[35] The same correlation function enters in the calculations of the third-order nonlinear susceptibility (to order E^3), $\chi^{(3)}$.[32] Numerous nonlinear optical measurements can be interpreted in terms of $\chi^{(3)}$. Fluorescence, coherent and spontaneous Raman, hole-burning, pump–probe, and four-wave mixing are a few examples of optical measurements related to $\chi^{(3)}$. The expansions can be carried out to higher orders, and in general, the rate to order V^{2n} is related to $\chi^{(2n-1)}$.

This connection establishes a fundamental link between the dynamics of rate processes and nonlinear optical measurements and provides a novel way of interpreting both types of experiments in a unified way. Optical measurements constitute the most sensitive and accurate probes for solvation dynamics. The relations presented in this Account allow the direct use of information obtained in optical measurements, in the calculation of rate processes. An example is the phenomenological identification of rotational diffusion rates obtained by fluorescence depolarization, as the relevant solvent time scale in adiabatic rate theories.[4,5,15,16] The present theory establishes such relations in a very profound way. In addition, the theoretical methodology used in calculating optical line shapes is well developed and provides a good understanding of solvent *dephasing* processes, which control the spectral shapes and line widths. The present relations allow the use of the same methods and concepts in the intepretation of rate processes as well.

II. Molecular Dynamics in Liouville Space

We consider a reactive molecular system undergoing a rate process such as electron transfer or isomerization in solution. The reaction rate can be calculated by using an *adiabatic* formulation, whereby the electronic energy is calculated for every nuclear configuration. This results in a single potential surface that depends parametrically on the nuclear configuration. The rate process is then described as a motion of the system on this surface. The Kramers and the Smoluchowski equations are based on this viewpoint.[14,17] Alternatively, the rate process can be described by using a *nonadiabatic* picture, in which we consider a two-level electronic system, $|a\rangle$ and $|b\rangle$, representing reactants and products, respectively, that are coupled by a nonadiabatic coupling V. It is the latter approach that we adopt in this Account, since it provides the best insight on the relationship between rate processes and nonlinear optical measurements. In the strong coupling limit our results agree with those derived from adiabatic models.

We start our analysis by considering a rate process involving a molecular system with two electronic levels ($|a\rangle$ and $|b\rangle$) in a solvent. The total Hamiltonian is

$$H = H_0 + H_{int} \tag{II-1}$$

where

$$H_0 = |a\rangle H_a \langle a| + |b\rangle H_b \langle b| \tag{II-2a}$$

$$H_{int} = V(|a\rangle\langle b| + |b\rangle\langle a|) \tag{II-2b}$$

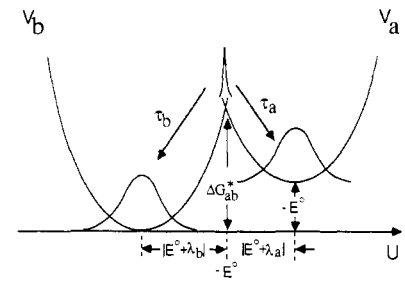

Figure 1. Solvation dynamics during a rate process. U is the solvation coordinate. V_a and V_b denote the adiabatic potential surfaces while $\lambda_a = \langle U\rho_a\rangle$ and $\lambda_b = \langle U\rho_b\rangle$ are the solvent reorganization energies for reactant and product, respectively. $E°$ is the endothermicity; ΔG_{ab}^* is the activation free energy for the forward ($|a\rangle$ to $|b\rangle$) reaction. The solvent time scales τ_a and τ_b characterize the relaxation of a solvent fluctuation at the transition state (curve crossing $U = -E°$) in the reactant and the product adiabatic surfaces, respectively. Harmonic free energy surfaces are used in this figure. We have chosen the origin of the solvation coordinate to be at the crossing point so that $\lambda_a > 0$ and $\lambda_b < 0$. In the perturbative limit, the rate depends only on the single Marcus reorganization energy parameter $2\lambda = |\lambda_a - \lambda_b|$.

Here H_a and H_b are the adiabatic Hamiltonians representing *nuclear* degrees of freedom (both intramolecular and solvent) and V is the nonadiabatic coupling between the two reacting species (Figure 1). The dynamics of the system may be calculated by starting with the Liouville equation for its density matrix $\hat{\rho}$,

$$\frac{d\hat{\rho}}{dt} = -i[H_0,\hat{\rho}] - i[H_{int},\hat{\rho}] \tag{II-3a}$$

and assuming that initially the system is in thermal equilibrium within the $|a\rangle$ state; i.e., $\hat{\rho}(0) = |a\rangle\rho_a\langle a|$, with

$$\rho_j \equiv \exp(-H_j/kT)/[Tr\ \exp(-H_j/kT)] \qquad j = a, b \tag{II-3b}$$

For brevity we set $\hbar = 1$ in this Account, except in the final expressions for the rates. The probability of the system to be in the state $|a\rangle$ may be obtained by calculating the diagonal density matrix element $\hat{\rho}_{aa}$ and tracing it over all nuclear (intramolecular and solvent) degrees of freedom. This may be done by using standard projection operator techniques in Liouville space.[35] We then obtain an exact formal expression for the reaction rate constant K. We have expanded the rate perturbatively to fourth order in the nonadiabatic coupling ($K = C_2V^2 - C_4V^4 + ...$) and constructed a Pade approximant which provides a partial summation of the series to infinite order, resulting in[35]

$$K = \frac{V^2C_2}{1 + V^2(C_4/C_2)} \tag{II-4}$$

Rate expressions with the same rational dependence on the nonadiabatic coupling V were obtained previously by several authors.[8-11] C_2 is given by

$$C_2 = 2\ \mathrm{Re} \int_0^\infty dt_1\ J(t_1) \tag{II-5}$$

where Re denotes the real part and

$$J(t_1) = \langle[\exp(-iH_bt_1)\rho_a \exp(iH_at_1)]\rangle \equiv \langle G_{ba}(t_1)\rho_a\rangle \tag{II-6}$$

$J(t_1)$ is calculated by starting with the equilibrium density matrix ρ_a, propagating it from the left and the right with the Hamiltonians H_b and H_a, respectively,

(36) *The Photosynthetic Bacterial Reaction Center*; Breton, J., Vermeglio, A., Eds.; Plenum: New York, 1988.

for a time period t_1, and then taking a trace. The angular brackets $\langle ... \rangle$ introduced in eq II-6 denote a trace over all nuclear (solvent and molecular) degrees of freedom. $G_{mn}(t)$ is a Liouville-space Green function, defined by its action on an arbitrary operator A:

$$G_{mn}(t)A \equiv \exp(-iH_m t)A \exp(iH_n t) \qquad m, n = \text{a, b} \tag{II-7}$$

The fourth-order contribution to the rate constant (eq II-4) is given by

$$C_4 = 2\,\mathrm{Re} \int_0^\infty dt_1 \int_0^\infty dt_2 \int_0^\infty dt_3\, [R(t_3,t_2,t_1) - R(t_3,\infty,t_1)] \tag{II-8}$$

$R(t_3,t_2,t_1)$ is calculated in an analogous way to $J(t_1)$ by starting with ρ_a, propagating it for three consecutive time periods t_1, t_2, and t_3 with various choices of propagation with H_a and H_b from the left and the right, and then taking a trace, i.e.,

$$R(t_3,t_2,t_1) = \sum_{j=1}^{4} R_j(t_3,t_2,t_1) \tag{II-9a}$$

$$R_1(t_3,t_2,t_1) = \langle G_{ba}(t_3)\, G_{bb}(t_2)\, G_{ba}(t_1)\rho_a \rangle \tag{II-9b}$$

$$R_2(t_3,t_2,t_1) = \langle G_{ba}(t_3)\, G_{bb}(t_2)\, G_{ab}(t_1)\rho_a \rangle \tag{II-9c}$$

$$R_3(t_3,t_2,t_1) = \langle G_{ba}(t_3)\, G_{aa}(t_2)\, G_{ab}(t_1)\rho_a \rangle \tag{II-9d}$$

$$R_4(t_3,t_2,t_1) = \langle G_{ba}(t_3)\, G_{aa}(t_2)\, G_{ba}(t_1)\rho_a \rangle \tag{II-9e}$$

Expressions similar to eq II-5 and II-8 can be derived for the higher order terms in the expansion (C_6, C_8, etc.) without a major difficulty. In general, C_{2n} will contain a product of $2n - 1$ Liouville-space Green functions $G_{mn}(t)$. For the subsequent analysis presented in this Account, we need not write these higher order expressions explicitly. The physical significance of $J(t_1)$ and $R(t_3,t_2,t_1)$ will further be clarified in the next section, following the introduction of a semiclassical procedure for their evaluation.

We shall consider now the analogous model system for linear and nonlinear optical spectroscopy. Consider a molecule with a ground electronic state $|a\rangle$ and a single excited electronic state $|b\rangle$, interacting with the electromagnetic field. The Hamiltonian is given by eq II-1, but H_{int} represents the interaction with a classical electromagnetic field $E(\mathbf{r},t)$:

$$H_{int} = -\mu E(\mathbf{r},t)(|a\rangle\langle b| + |b\rangle\langle a|) \tag{II-10}$$

Here H_a and H_b represent the Hamiltonians for the intramolecular (vibration, rotation) and for the solvent degrees of freedom, when the system is in the electronic states $|a\rangle$ and $|b\rangle$, respectively, and μ is the electronic transition dipole matrix element. The optical properties of the system may be related to the time-dependent polarization $P(\mathbf{r},t)$. The polarization is usually expanded in a Taylor series in E:[32]

$$P(\mathbf{r},t) = P^{(1)}(\mathbf{r},t) + P^{(2)}(\mathbf{r},t) + P^{(3)}(\mathbf{r},t) + ... \tag{II-11}$$

$P^{(1)}$ is related to the linear optical properties, whereas $P^{(2)}$, $P^{(3)}$, etc., constitute nonlinear contributions. In an isotropic medium, $P^{(2)} = 0$; we shall therefore focus on $P^{(1)}$ and $P^{(3)}$. The polarization is calculated by taking the expectation value of the dipole operator $\hat{\mu} \equiv \mu(|a\rangle\langle b| + |b\rangle\langle a|)$, after the density matrix $\hat{\rho}$ is calculated to the desired order. $P^{(1)}$ is given by a convolution of the electromagnetic field E and the *linear response function*, $-2|\mu|^2$ Im $J(t_1)$, where $J(t_1)$ is given by eq II-6,

$$P^{(1)}(\mathbf{r},t) = -2|\mu|^2\,\mathrm{Im} \int_0^\infty dt_1\, J(t_1)\, E(\mathbf{r},t-t_1) \tag{II-12}$$

Here Im denotes the imaginary part. Similarly $P^{(3)}$ is given by a triple convolution of the electromagnetic field and the third-order *nonlinear response function*, $2|\mu|^4$ Im $R(t_3,t_2,t_1)$, where $R(t_3,t_2,t_1)$ is given by eq II-9:

$$P^{(3)}(\mathbf{r},t) = 2|\mu|^4\,\mathrm{Im} \int_0^\infty dt_1 \int_0^\infty dt_2 \int_0^\infty dt_3\, R(t_3,t_2,t_1)\, E(\mathbf{r},t-t_1-t_2-t_3)\, E(\mathbf{r},t-t_2-t_3)\, E(\mathbf{r},t-t_3) \tag{II-13}$$

Equation II-12 implies that the system interacts once with the electromagnetic field at time $t - t_1$. Its subsequent evolution for a period t_1 is then given by the linear response function. $P^{(1)}$ at time t is obtained by performing an integration over all possible values of t_1. Similarly, in eq II-13, the system interacts three times with the electromagnetic field at times $t - t_1 - t_2 - t_3$, $t - t_2 - t_3$, and $t - t_3$. The nonlinear response function $R(t_3,t_2,t_1)$ describes the time evolution between these interactions and from time $t - t_3$ to t. t_1, t_2, and t_3 are the time intervals between successive interactions. The integrations over all possible values of t_1, t_2, and t_3 result in the third-order nonlinear polarization at time t. Equations II-12 and II-13 allow for an arbitrary temporal profile of $E(\mathbf{r},t)$ and are valid for pulsed as well as steady-state experiments. In a steady-state experiment we take $E(\mathbf{r},t)$ to be the sum of a few monochromatic fields. $P^{(1)}$ and $P^{(3)}$ are then related to the *optical susceptibilities* $\chi^{(1)}$ and $\chi^{(3)}$, respectively.[32]

The formal expressions presented here establish a fundamental connection between the calculation of rate constant (eq II-4 together with II-5 and II-8) and the optical polarization (eq II-12 and II-13). The reaction rates are expressed in terms of the real part of the dynamical quantities $J(t_1)$ and $R(t_3,t_2,t_1)$, whereas the optical polarization is related to the imaginary part of these dynamical quantities. It should be emphasized, however, that the two states $|a\rangle$ and $|b\rangle$ involved in an optical measurement are usually different from those participating in a rate process (electron transfer or isomerization) in the same chromophore. Their electronic charge distribution and coupling to the solvent could therefore be very different. Consequently, the correlation functions $J(t_1)$ and $R(t_3,t_2,t_1)$ may be very different in both cases. Nevertheless, the way the solvent couples with optical and rate processes is formally identical, and the powerful theoretical methods and concepts, such as dephasing processes developed for the interpretation of optical spectroscopy, can be readily used in the description of rate processes using the present formulation. In the remainder of this Account, we shall apply the present formal expressions to analyze the role of solvation dynamics in electron transfer and in the optical measurements (absorption, fluorescence, and pump–probe) of a chromophore in a polar solvent environment. For clarity we consider only the contribution of solvent modes to $J(t_1)$ and $R(t_3,t_2,t_1)$ and do not include intramolecular nuclear degrees of freedom (vibrations and rotations).

III. Semiclassical Approximation for Solvation Dynamics

In this section, we develop a general yet very simple semiclassical approximation scheme for the calculation

of the solvent correlation functions $J(t_1)$ and $R(t_3,t_2,t_1)$. The present approach provides useful expressions for these correlation functions and offers a tremendous insight regarding the important factors that affect the dynamics of reaction rates and optical line shapes. Consider the various Liouville-space Green functions $G_{mn}(t)$ that enter in eq II-6 and II-9. The Green functions with $m = n$, $G_{aa}(t_2)$ and $G_{bb}(t_2)$, represent the evolution of the diagonal elements of the density matrix (*level populations*) whose time evolution from the left and from the right is with the same Hamiltonian. On the other hand, $G_{ba}(t)$ and $G_{ab}(t)$, with $t = t_1$ or t_3, represent the time evolution of *molecular coherences* (off-diagonal elements of the density matrix); their time evolution from the left and from the right is with different Hamiltonians. The semiclassical approximation is obtained by approximating the Liouville-space Green function corresponding to coherences as

$$G_{ba}(t) = G_{ab}^{\dagger}(t) \cong \exp[-i(U + E^{\circ})t] \quad \text{(III-1)}$$

where $U \equiv H_b - H_a - E^{\circ}$ is the *solvation coordinate*. $E^{\circ} = \hbar\omega_{ba}$ is the energy difference between the potential minima of H_a and H_b. In a rate process this is the reaction free energy (denoted E°), whereas in an optical process this is the fundamental 0–0 transition energy (denoted $\hbar\omega_{ba}$). This approximation may be derived by assuming that H_a and H_b commute, resulting in the cancellation of the solvent nuclear kinetic energy. The semiclassical approximation is expected to hold at high temperatures and is known in the theory of spectral line shapes as the static or the statistical limit.[37] The motions and fluctuation properties of solvent degrees of freedom as collectively appear in U play a major role in controlling the spectral broadening as well as the dynamics of electron transfer. Our semiclassical approximation for the response functions is obtained by substituting eq III-1 for $G_{ba}(t)$ and its Hermitian conjugate $G_{ab}(t)$ in eq II-6 and II-9.

At this point we should make a few comments to clarify why we are using the semiclassical approximation for the coherences (G_{ba} and G_{ab}) and not for the populations (G_{aa} and G_{bb}). Coherences in condensed phases are usually subject to fast *dephasing* processes resulting from the solvent motions that destroy the phase of the density matrix elements $\hat{\rho}_{ba}$ and $\hat{\rho}_{ab}$. Consequently, the coherence Green functions are expected to decay rapidly, and the relevant time scales t_1 and t_3 that enter into eq II-6 and II-9 are of the order of the dephasing time scale. The latter is typically in the femtosecond range, as can be seen from the line widths of optical transitions in solution. We thus need to evaluate $G_{ba}(t)$ and $G_{ab}(t)$ for very short times, over which the solvent nuclei are practically stationary, and a semiclassical approximation is justified. Pure dephasing processes do not affect the diagonal elements of the density matrix (populations), so the typical time scales for t_2 in eq II-9 are of the order of the lifetime of the electronic states, which may be much longer (typically in the nanosecond to subpicosecond range). It is therefore reasonable to ignore the solvent nuclear kinetic energy when the system is in a coherence (the t_1 and t_3 intervals) but not when it is in a population (t_2). In order to express our results in a compact form, we introduce two auxiliary quantities. The first is the probability distribution of the solvation coordinate U when the system is in the state j:

$$\sigma_j(x) \equiv \langle \delta(x-U)\rho_j \rangle \qquad j = a, b \quad \text{(III-2)}$$

The second quantity is the conditional probability for the solvation coordinate to have the value x at time t, given that it had the value y at $t = 0$ and that the system is in the state j, i.e.,

$$W_j(x,t;y) \equiv [\sigma_a(y)]^{-1}\langle \delta[x-U_j(t)]\ \delta(y-U)\rho_a \rangle \quad \text{(III-3)}$$

where

$$U_j(t) = \exp(iH_jt)U\exp(-iH_jt) \qquad j = a, b \quad \text{(III-4)}$$

Note that, by definition, $W_j(x,0;y) = \delta(x-y)$ and $W_j(x,\infty;y) = \sigma_j(x)$.

We shall now apply the semiclassical approximation to optical line shapes. Within the semiclassical approximation, we view the solvation coordinate simply as a classical function of the solvent degrees of freedom (rather than an operator). A photon ω may be absorbed or emitted only when the solvation coordinate has the value $U = \omega - \omega_{ba}$. This is the classical Franck–Condon principle.[38] The absorption spectrum at frequency ω is then proportional to the probability of the solvation coordinate to have the value $\omega - \omega_{ba}$ when the system is in the $|a\rangle$ state. This probability is $\sigma_a(\omega-\omega_{ba})$. Similarly, $\sigma_b(\omega-\omega_{ba})$ is the emission (fluorescence) spectrum in a steady-state experiment when the radiative lifetime is long compared with the solvent relaxation, so that the emission is from an excited state where the solvent is fully relaxed. We next consider two time-resolved spectroscopic techniques that are commonly used in the studies of solvation: fluorescence and hole-burning (pump–probe) spectroscopies.[21-25,34] Both measurements are related to $P^{(3)}$ and start with the application of a short pump pulse centered at $t = 0$ with frequency ω_1. In a time-resolved fluorescence measurement, the solvation dynamics when the solute is in the excited electronic state $|b\rangle$ are probed by collecting a spontaneously emitted photon with frequency ω_2 at time t. The fluorescence signal may be expressed in terms of the response functions R_1 and R_2 introduced in section II and is given by[33,34]

$$S_{FL}(\omega_1,\omega_2,t) = \omega_1\omega_2^3 W_b(\omega_2-\omega_{ba},t;\omega_1-\omega_{ba})\ \sigma_a(\omega_1-\omega_{ba}) \quad \text{(III-5)}$$

Equation III-5 can be interpreted as follows. $\sigma_a(\omega_1-\omega_{ba})$ is the rate of absorbing a photon ω_1 by the system. $W_b(\omega_2-\omega_{ba},t;\omega_1-\omega_{ba})$ is the conditional probability of the solvation coordinate to have the value $U = \omega_2 - \omega_{ba}$ at time t given that it had the value $U = \omega_1 - \omega_{ba}$ at $t = 0$. The rate of emitting an ω_2 photon at time t following the absorption of an ω_1 photon at $t = 0$ is thus proportional to the product of σ_a and W_b.

In an ultrafast pump–probe (hole-burning) measurement, the absorption spectrum is measured with a probe pulse that is delayed relative to the pump pulse by time t. The hole-burning line shape $S_{HB}(\omega_1,\omega_2,t)$ is defined as the difference between the absorption coefficient at ω_2 in the absence of a pump pulse and the absorption coefficient at ω_2 measured with a probe pulse that follows a pump pulse. Since the hole-burning line shape is proportional to the population difference between the two electronic states, the solvation dynamics

(37) Breene, R. G. *Theories of Spectral Lineshapes*; Wiley: New York, 1981.

(38) Lax, M. *J. Chem. Phys.* **1952**, *20*, 1752.

in both the excited state (with R_1 and R_2) and the ground state (with R_3 and R_4) enter in $S_{HB}(\omega_1,\omega_2,t)$. We then get[33,34]

$$S_{HB}(\omega_1,\omega_2,t) = \omega_1\omega_2[W_b(\omega_2-\omega_{ba},t;\omega_1-\omega_{ba}) + W_a(\omega_2-\omega_{ba},t;\omega_1-\omega_{ba})]\sigma_a(\omega_1-\omega_{ba}) \quad \text{(III-6)}$$

Equation III-5 and III-6 were derived by assuming that both the pump and the probe pulses are short compared to the time scales of the orientational relaxation of the solvent. Let us consider now the origin and the physical interpretation of the two contributions to the hole-burning spectrum. In this experiment the excitation pulse selects a group of molecules in the ground state whose solvation coordinate is around $U = \omega_1 - \omega_{ba}$ and transfers them to the excited state, thus creating a "particle" in the excited state and a "hole" in the ground state. W_b results from the R_1 and R_2 terms and their complex conjugates. In these pathways, the system is in the electronically excited state $|b\rangle$ during the time interval t_2, where the solvation dynamics takes place. The solvation coordinate will attain the limiting distribution determined by ρ_b as $t_2 \rightarrow \infty$. W_b represents, therefore, the excited "particle" dynamics as discussed previously for the fluorescence spectra. W_a, on the other hand, results from pathways R_3 and R_4 and their complex conjugates, in which the system is back in the ground state $|a\rangle$ during the t_2 time interval. W_a represents "holes" in the ground-state distribution. The solvation dynamics underlying W_a corresponds to the relaxation of the solvation coordinate to attain the equilibrium distribution determined by ρ_a. Since the probe absorption spectrum is sensitive to the population difference between the ground and the excited states, it depends on both W_b and W_a.

It should be noted that a more general theory of pump–probe spectroscopy may be required in order to account for the most recent femtosecond experiments in which coherent nuclear motions (quantum beats) are produced in real time.[19,20,22-24] The necessary generalizations of eq III-5 and III-6 include the use of more microscopic models for the solvation dynamics, avoiding the static approximation (eq III-1) and including the quantum dynamics instead, and the incorporation of molecular vibrations using their phase space distributions. In addition, since in many of the current femtosecond experiments the pump and the probe may overlap in time, it is necessary to allow for all possible time orderings of the pump with respect to the probe. (In the present theory, we assume that the pump acts first and the probe second.) All these generalizations can be incorporated by starting with eq II-13.[26,32]

We next turn to the rate constant (eq II-4). When the semiclassical approximation eq III-1 is substituted in eq II-6 and II-9, and the integrations over t_1 and t_3 in eq II-5 and II-8 are performed, the reaction rate assumes the form

$$K = \frac{2\pi(V^2/\hbar)\sigma_a(-E^\circ)}{1 + 2\pi(V^2/\hbar)\sigma_a(-E^\circ)(\tau_a + \tau_b)} \quad \text{(III-7)}$$

$$\tau_j = [\sigma_a(-E^\circ)]^{-1}\int_0^\infty dt\,[W_j(-E^\circ,t;-E^\circ) - W_j(-E^\circ,\infty;-E^\circ)] \qquad j = a, b \quad \text{(III-8)}$$

The nature of the rate process is determined by the *adiabaticity parameter* $\nu \equiv 2\pi(V^2/\hbar)\sigma_a(-E^\circ)(\tau_a + \tau_b)$. When $\nu \ll 1$, the reaction is nonadiabatic and we have $K_{NA} = 2\pi(V^2/\hbar)\sigma_a(-E^\circ)$. In the opposite limit, $\nu \gg 1$, the reaction is adiabatic and the rate is given by $K_{AD} = (\tau_a + \tau_b)^{-1}$.

The present expression for the rate constant as well as the adiabaticity parameters has been derived and discussed previously by many authors.[8-11,17] The nonadiabatic rate expression, which may be simply obtained from the Fermi golden rule, was developed by Levich and co-workers for Debye solvents[39] and then generalized to an arbitrary solvent by Ovchinnikov and Ovchinnikova[40] and by Zusman and Helman.[10] The early works of Hopfield,[6] Jortner,[7] and co-workers also focused on the nonadiabatic limit. Zusman has used a Markovian stochastic Liouville equation to derive a rate expression that interpolates between the adiabatic and the nonadiabatic limits. When the Debye model for the solvent is used, eq III-7 reduces to these earlier results. The adiabatic rate given here was also derived by Hynes,[17] Sumi and Marcus,[8] and Rips and Jortner[9] for the Debye model. The derivation of Hynes is based on formulating the rate constant in terms of a flux correlation function, starting with an adiabatic (single potential surface) picture. The present derivation, which starts with the opposite (nonadiabatic) representation and is based on the evaluation of the nonlinear response function, provides an unconventional viewpoint for interpreting the expression and, most importantly, establishes the connection with nonlinear optical spectroscopy. In the semiclassical (static) approximation, the nonadiabatic rate depends on the value of $\sigma_a(x)$ at one point $x = -E^\circ$. That point is the curve crossing (the transition state) (Figure 1). K_{NA} could be derived by making a static approximation starting with the Fermi golden rule. When the adiabaticity parameter is sufficiently large, the reaction becomes adiabatic, and the rate constant is equal to $(\tau_a + \tau_b)^{-1}$. τ_a and τ_b *are the characteristic solvent time scales which control the adiabaticity of the rate process.* Let us have a closer examination of the physical significance of these time scales. τ_b results from a combination of R_1 and R_2 that passes through an intermediate state $\hat{\rho}_{bb}$ as shown by $G_{bb}(t_2)$ in eq II-9. During the t_2 interval the reactant has changed into the product, but the solvation coordinate U is not in thermal equilibrium with the product $|b\rangle$. It then undergoes relaxation to equilibrium during the t_2 period as given by $G_{bb}(t_2)$ in eq II-9b and II-9c. When it reaches equilibrium ($t_2 \rightarrow \infty$), the integrand in eq II-8 vanishes, and it does not contribute to the rate any more. The time scale for this equilibration process is τ_b. τ_a results from the combination of R_3 and R_4 that passes through an intermediate state $\hat{\rho}_{aa}$ as shown by $G_{aa}(t_2)$ in eq II-9. This represents the back reaction processes in which the system has passed through the transition state and has returned back to the reactant $|a\rangle$. Again, the solvation coordinate undergoing this process is not in thermal equilibrium with the reactant, and it relaxes to equilibrium during the t_2 period, as given by $G_{aa}(t_2)$. The time scale for this relaxation process is τ_a. When this relaxation is completed, the

(39) Levich, V. In *Physical Chemistry, an Advanced Treatise*; Eyring, H., Henderson, D., Jost, W., Ed.; Academic Press: New York, 1970; Vol. 9B.

(40) Ovchinnikov, A. A.; Ovchinnikova, M. Y. *Sov. Phys.—JETP (Engl. Transl.)* **1969**, *29*, 688.

integrand in eq II-8 vanishes and does not contribute to the rate. τ_b is thus the average time it takes for a solvent fluctuation at the transition state ($U = -E°$) to relax to thermal equilibrium in the product well $|b\rangle$, whereas τ_a is the average time it takes for the same fluctuation to relax to thermal equilibrium in the reactant well $|a\rangle$. This is represented schematically in Figure 1. τ_b is determined by the same solvation dynamics that controls W_b, whereas τ_a is related to the solvation dynamics that controls W_a. If these time scales are fast, the adiabaticity parameter ν vanishes and the rate is nonadiabatic. As the solvent time scales become longer, ν increases, and a nonadiabatic rate will eventually turn adiabatic, with a rate equal to the proper inverse solvent time scale. The transition from the nonadiabatic to the adiabatic limit is therefore a result of the finite relaxation time of the solvent, which results in a change of the distribution of the solvation coordinate U at the transition state $U = -E°$ during the course of the rate process. These results are in full agreement with the established predictions of reaction rate theories.[1-10,17] It should be stressed that in eq III-7 and III-8, we did not have to assume a priori that the reaction takes place at the transition-state configuration $U = -E°$. This is rather a direct consequence of the semiclassical approximation.

Our results provide a unique insight on the dynamics of optical and rate processes. The fluorescence spectrum depends on solvation dynamics when the system is electronically excited, whereas the pump–probe spectrum contains both excited-state and ground-state dynamics.[34] The nonlinear optical spectra probe the conditional probabilities $W_j(x,t;y)$ (j = a, b) directly. By varying t, ω_1, and ω_2, we directly measure W_j as a function of x, t, and y. In contrast, the timescales τ_a and τ_b that enter in the rate expression are averages of the appropriate W_j functions for a single value of x and y, $x = y = -E°$, and integrated over time. The information regarding solvation dynamics necessary to calculate reaction rates is therefore much more averaged than the information that could be obtained from fluorescence and hole-burning measurements. We reiterate that the solvent quantities σ_j and W_j entering into the calculations of the rate constant (eq III-7 and III-8) are in general different from those appearing in the hole-burning and the fluorescence measurements (eq III-5–III-8), since different electronic states are involved. In the next section we show that when certain approximations are made, the solvation dynamics is identical in both cases.

The validity of the semiclassical approximation is intimately connected to the influence of *pure dephasing processes* that destroy optical coherences during the time intervals t_1 and t_3 and allow us to use a short time approximation. Dephasing processes play an important role in spectroscopy and in dynamical line shape analysis.[32,37] The present formulation introduces this concept to the analysis of rate processes as well and provides a new way of interpreting rate processes. It is interesting to note that the form of the rate constant and the transition from the nonadiabatic to the adiabatic regime is strikingly analogous to the saturation of spectral line shapes in a strong radiation field (the Karplus–Schwinger line shape),[41] where V is replaced by the Rabi frequency $|\mu E|$. This is another beautiful manifestation of the intimate relationship between nonlinear optics and the dynamics of rate processes.

IV. Ultrafast Spectroscopy and Electron Transfer in Polar Solvents

Dielectric fluctuations in polar solvents play a crucial role in electron transfer and optical spectroscopy.[8,34] Assuming electrostatic interaction between the solute and the solvent polarization, we have for the solvation coordinate

$$U = -\int \mathrm{d}\mathbf{r}\,[D_b(\mathbf{r}) - D_a(\mathbf{r})]P(\mathbf{r}) \qquad j = \mathrm{a, b} \qquad \text{(IV-1)}$$

where the electric fields at position $\mathbf{r}$ created by the system in reactant and product are denoted $D_a(\mathbf{r})$ and $D_b(\mathbf{r})$, respectively, and $P(\mathbf{r})$ is the solvent polarization. We have evaluated the solvent quantities (eq III-2 and III-3) to second order in the solvent–solute interaction, assuming Gaussian statistics of solvent fluctuations, resulting in[35]

$$\sigma_a(x) = \frac{1}{(4\pi\lambda k_B T)^{1/2}} \exp\left[-\frac{(x-\lambda)^2}{4\lambda k_B T}\right] \qquad \text{(IV-2)}$$

$$W_a(x,t;y) = \{4\pi\lambda k_B T[1 - M^2(t)]\}^{-1/2} \exp\left\{-\frac{[x - \lambda - M(t)(y-\lambda)]^2}{4\lambda k_B T[1 - M^2(t)]}\right\} \qquad \text{(IV-3)}$$

$\sigma_b(x)$ and $W_b(x,t;y)$ are given by the same expressions by replacing $x - \lambda$ and $y - \lambda$ with $x + \lambda$ and $y + \lambda$, respectively. The solvation information entering eq IV-2 and IV-3 is contained in a single static parameter λ and a single dynamical quantity $M(t)$. $2\lambda \equiv \langle U\rho_a\rangle - \langle U\rho_b\rangle$ is the solvent reorganization energy[8,35] due to the change in the molecular configuration from reactant to product. $M(t) \equiv [\langle U(t)U\rangle - \langle U\rangle^2]/[\langle U^2\rangle - \langle U\rangle^2]$ is a normalized solvent correlation function, with $M(0) = 1$ and $M(\infty) = 0$.

The semiclassical formulation developed in section II showed how molecular rate processes and nonlinear optical line shapes may be expressed in terms of the solvent quantities $\sigma_j(x)$ and $W_j(x,t;y)$, which depend on λ and $M(t)$. In optical measurements, 2λ represent the static Stokes shift while $M(t)$ is the normalized dynamical Stokes shift function.[21,33,34] Using eq IV-1, λ and $M(t)$ can be expressed in terms of the solvent polarization correlation function, $C_{pp}(\mathbf{r}-\mathbf{r}',t)$, and the difference between the electric fields, D_a and D_b. $C_{pp}(\mathbf{r}-\mathbf{r}',t)$ can further be related, by using the fluctuation–dissipation theorem, to the wavevector- and frequency-dependent solvent dielectric function $\epsilon(\mathbf{k},\omega)$.[42] The dielectric function is usually known from macroscopic (long wavelength) measurements that yield only the $\mathbf{k} = 0$ component of $\epsilon(\mathbf{k},\omega)$. If the wavevector dependence of ϵ is ignored and we substituted $\epsilon(\omega) \equiv \epsilon(\mathbf{k} = 0,\omega)$ for $\epsilon(\mathbf{k},\omega)$, we obtain the commonly used dielectric continuum (long wavelength) approximation[34,35]

$$\lambda = r^{-3}|\mu_a - \mu_b|^2[1/\epsilon_\infty - 1/\epsilon_0] \qquad \text{(IV-4a)}$$

$$M(t) = \frac{1}{2\pi i}\int_{-\infty}^{\infty}\frac{\mathrm{d}\omega}{\omega}\exp(i\omega t)\frac{1/\epsilon(\omega) - 1/\epsilon_0}{1/\epsilon_\infty - 1/\epsilon_0} \qquad \text{(IV-4b)}$$

(41) Karplus, R.; Schwinger, M. J. *Phys. Rev.* **1948**, *73*, 1020.

(42) Loring, R. F.; Mukamel, S. *J. Chem. Phys.* **1987**, *87*, 1272.

where ϵ_0 is the static ($\omega = 0$) and ϵ_∞ is the high-frequency (optical) value of the solvent dielectric function. In eq IV-4a, we have evaluated the fields D_a and D_b by assuming that the system has permanent dipoles μ_a and μ_b in the a and b states, respectively. r is the effective molecular size (hard-sphere radius).[34] Note that in this case λ depends strongly on the nature of the electronic system whereas $M(t)$ depends only on the solvent. Let us consider a typical form for the dielectric function that holds for a large number of solvents, i.e., the Cole–Davidson form:[43]

$$\epsilon(\omega) = \epsilon_\infty + \frac{(\epsilon_0 - \epsilon_\infty)}{(1 + i\omega\tau_0)^\beta} \qquad \text{(IV-5)}$$

Equation IV-5 represents a solvent with a distribution of dielectric relaxation time scales, and β and τ_0 are two parameters characterizing this distribution. (τ_0 is a typical solvent time scale, and β controls the width of the distribution.) The Debye model for the dielectric function is given by eq IV-5 with $\beta = 1$. For this model in the continuum ($\mathbf{k} = 0$) approximation, the system has a single dielectric relaxation time τ_0. We then get $M(t) = \exp(-t/\tau_L)$ with τ_L being the longitudinal solvent relaxation time $\tau_L = \tau_0(\epsilon_\infty/\epsilon_0)$. It is interesting to note that, for the Debye model, the time scales of the Stokes shift and the line broadening in hole-burning and in fluorescence, and the solvent time scales relevant to the rate (τ_a and τ_b) for small barriers, are all equal to τ_L.[35] This is a special characteristic of the Debye continuum model. In general, the solvent has several time scales; $M(t)$ as displayed in fluorescence and hole-burning measurements will show directly these various time scales, whereas τ_a and τ_b, which appear in the rate constant (eq III-7), will be some weighted average of these time scales. It should further be noted that even in a Debye solvent we expect to have a multitude of time scales related to the dynamics of the various solvation shells. The incorporation of solvation shell structure may be made in the present formulation by considering the complete frequency- and wavevector-dependent dielectric function.[42,44] This is essential in order to calculate the multiple relevant solvent time scales that are experimentally observed in, e.g., time-resolved fluorescence measurements.[21,44]

We have calculated fluorescence and pump–probe (hole-burning) line shapes of a polar solute in a Debye model solvent at 247 K with $\epsilon_0 = 33.5$, $\epsilon_\infty = 4.8$, and $\tau_L = 150$ ps.[34] In these calculations we have also included intramolecular vibrations by writing $J(t_1)$ and $R(t_3,t_2,t_1)$ as products of a solvation term and an intramolecular term, which may be evaluated analytically for harmonic molecules.[32-34] In Figure 2 we display the calculated time-resolved hole-burning spectrum of the retinal chromophore in bacteriorhodopsin, which has 29 optically active vibrational modes.[34] The frames show hole-burning spectra measured by probe pulse as successively longer delay times with respect to pump pulse. The hole-burning spectrum at 1 ps resembles a Raman spectrum, with distinct resonances when $\omega_1 - \omega_2$ equals the frequency difference of two vibronic states of the electronic ground state and the electronic excited state. The hole-burning spectrum for times short compared to τ_L shows substantial line narrowing relative to the steady-state spectrum, because the pump pulse is not sufficiently short to excite the entire inhomogeneous distribution of solute molecules. The pump pulse selects a subset of solute molecules and surrounding solvent environments whose transition frequencies are close to the excitation frequency, leaving particles in the excited electronic state and holes in the ground electronic state. For observation times much less than τ_L, the solvent is effectively static, and the hole-burning line shape is narrow. For observation times comparable to τ_L, the solvent around each particle and hole has begun to relax, and the spectrum broadens, and meanwhile the contribution of particles (W_b) displays a red shift. In the final frame, the steady-state hole-burning spectrum is reproduced (dashed line) for comparison with the spectrum at $t = \tau_L$.

We shall turn now to the calculation of electron-transfer rates in polar solvents with a Cole–Davidson dielectric function. In Figure 3, we present the rate constant (eq III-7) as a function of the solvent charac-

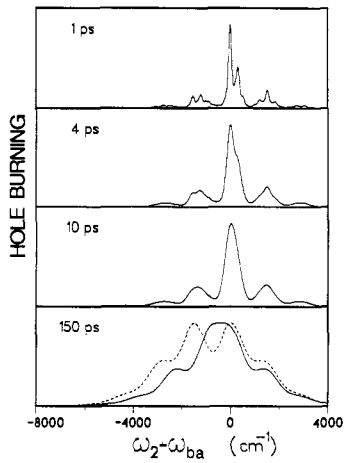

Figure 2. Time-resolved hole-burning spectra of a polyatomic solute in a Debye solvent at 247 K following a 1-ps excitation pulse. The longitudinal dielectric relaxation time, τ_L, is 150 ps. The model solute has the 29 Raman-active vibrational modes of the retinal chromophore in bacteriorhodopsin and undergoes rapid vibrational relaxation. The pump frequency is given by $\omega_1 = \omega_{ba} + \lambda + 1528$ cm^{-1}.

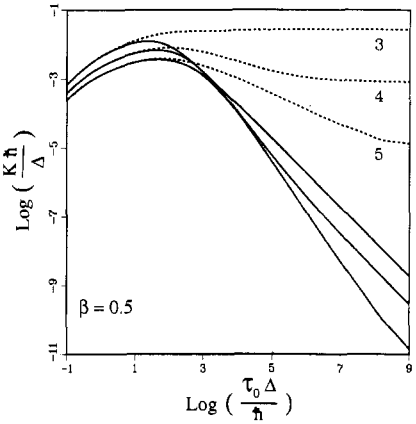

Figure 3. The logarithm (base 10) of the rate K (eq III-7) in units of $\Delta/\hbar$ is plotted as a function of log $(\tau_0\Delta/\hbar)$, where $\Delta = (2\lambda kT)^{1/2}$. $V = \Delta$. We assume $|E^\circ + \lambda|/\Delta > 1$ and neglect the back reaction by setting $\tau_a = 0$. The dashed curves show the logarithm of the nonadiabatic rate K_{NA} (setting $\tau_a = \tau_b = 0$). A Cole–Davidson solvent is used with $\beta = 0.5$, $\epsilon_0 = 64$, and $\epsilon_\infty = 4.1$. The different curves correspond to various values of $(E^\circ + \lambda)/\Delta$ as indicated.

(43) Bottcher, C. J. F.; Bordewijk, P. *Theory of Electric Polarization*; Elsevier: Amsterdam, 1978.
(44) Chandra, A.; Bagchi, B. *J. Chem. Phys.* **1989**, *90*, 1832.

teristic time scale τ_0 (eq IV-5). Large values of τ_0 correspond to high friction. In this case the reaction is adiabatic, and the rate decreases with increasing τ_0. When τ_0 is sufficiently small, the reaction is nonadiabatic and the rate is proportional to the line-shape function $\sigma_a(-E^\circ)$, which is motionally narrowed and assumes a Lorentzian form. Equation IV-2 does not hold in this case, and the rate is then proportional to the line width, which increases linearly with τ_0. The rate, when plotted vs τ_0, thus exhibits a maximum. This is analogous to the Kramers turnover curve.[14,15] The dashed curves show the nonadiabatic rates (the numerator of eq III-7), assuming the adiabaticity parameter $\nu = 0$. For small enough τ_0, the rate is nonadiabatic. As τ_0 increases, the nonadiabatic rate becomes independent of τ_0, since $\sigma(-E^\circ)$ assumes the Gaussian form. However, when τ_0 is sufficiently large, the rate eventually becomes adiabatic and decreases with τ_0, as shown by the solid curves.

This Account presents a general theoretical framework, based on the evolution of the density matrix, that allows the calculation of solvation dynamics and establishes a general fundamental connection between reaction rates and nonlinear optical processes in solution. Our theory of electron transfer in condensed phases interpolates between the nonadiabatic and the adiabatic limits. A new insight is provided for the transition from nonadiabatic to adiabatic rates, and the relevant solvent time scale that controls the adiabaticity is precisely defined. We have demonstrated how solvent correlation functions and dephasing rates extracted from linear and nonlinear optical measurements (absorption, fluorescence, hole-burning, and $\chi^{(3)}$) may be used to predict electron-transfer rates. A major goal of spectroscopic studies in condensed phases is to provide information that allows the prediction of reaction rates in the same solvent. When the solvent–solute interaction is treated perturbatively, and the dielectric continuum model is adopted for the solvent, then the solvation effect depends on a single static quantiy (the reorganization energy λ) and a single correlation function $M(t)$ (eq IV-4). λ is very sensitive to the nature of the electronic states involved in the process and is expected to be very different for electron transfer and optical measurements, even when using the same chromophore in the same solvent. $M(t)$, on the other hand, depends only on the solvent dielectric fluctuations. $M(t)$ obtained from, e.g., time-dependent Stokes shift measurements can then be used to predict electron-transfer rates in the same solvent. This simple prediction is a result of several simplifying approximations, particularly the dielectric continuum model for the solvent, which is of course a great oversimplification of the problem. The present theory points out how these approximations can be systematically improved and what static and dynamical quantities need to be calculated in order to develop a more microscopic description of solvation.

It is a pleasure to acknowledge the invaluable contributions of M. Sparpaglione and R. F. Loring to the work covered in this Account. The support of the Office of Naval Research, the National Science Foundation, and the donors of the Petroleum Research Fund, administered by the American Chemical Society, is gratefully acknowledged.